The membrane insertion of trichosanthin is membrane-surface-pH dependent

Xiao-feng XIA and Sen-fang SUI[1]

State Key Laboratory of Biomembranes, Department of Biological Sciences and Biotechnology, Tsinghua University, Beijing 100084, People's Republic of China

Trichosanthin (TCS) is the active component extracted from Tianhuafen, a traditional herbal medicine that has been used for abortion in China for centuries. It belongs to the type-I ribosome-inactivating protein (RIP) family and can inactivate the eukaryotic ribosome through its RNA N-glycosidase activity. Recent studies have shown TCS to be multifunctional, its pharmacological properties including immunomodulatory, anti-tumour and anti-HIV activities. The membrane-insertion property of TCS is thought to be essential for its physiological effect, for it must get across the membrane before it can enter the cytoplasm and exert its RIP function. In this paper, the membrane-insertion mechanism of TCS was studied. The monolayer experiment revealed that TCS's membrane-insertion ability was dependent on low pH. Fluorescence spectroscopy using 1-anilinonaphthalene-8-sulphonic acid as a probe showed that low pH may induce the conformational change of TCS that leads to the hydrophobic-site exposure, and the CD result showed that this conformational change did not alter its secondary structure. Such conformational change leads to an intermediate state, called the 'molten globular state' by previous investigators. The pH-dependent membrane insertion and conformational change were related by the fact that the optimal membrane-surface pH needed was the same for the two events. From these and other results, a membrane-insertion model was proposed.

Key words: conformational change, lipid–protein interaction, membrane surface pressure, molten globular state, ribosome-inactivating protein.

INTRODUCTION

Trichosanthin (TCS) is a toxic protein isolated from a Chinese herbal medicine, the root tuber of *Trichosanthes kirilowii maxim*, Cucurbitaceae (Tianhuafen) [1,2]. It has been used clinically in China to terminate early and mid-trimester pregnancies [3] and to treat trophoblastic tumours [4]. Its abortifacient activity is thought to be due to TCS binding to the trophoblastic syncytial layer and selectively killing cells [5]. Besides, TCS has been found to possess various pharmacological properties [6], the most remarkable among these being anti-HIV-infection activity [7–9]. In the early 1990s, TCS was applied in the treatment of patients with AIDS or AIDS-related complex in phase-I and -II studies [10–13].

TCS belongs to the type-I ribosome-inactivating protein (RIP) family [14], and consists of a single chain (27 kDa) that shows sequence homology to the A chain of many type-II RIPs [15,16]. TCS can inactivate ribosome by removing adenine-4324, the 4324th base of 28 S rRNA, via N-glycosidase activity [17,18]. This RIP activity was thought to account for its toxicity, which seriously restricted its clinical application for AIDS treatment.

Many studies have revealed the fact that membrane–protein interaction plays an important role in RIP's physiological effect [19,20]. These heterogeneous proteins must be translocated across the biological membrane before they can meet the ribosome and then inactivate it. TCS has been proved to be able to insert into the negatively charged phospholipid membrane in a pH-dependent manner [21]. But the mechanism of this membrane-insertion process remains unclear. In this paper, the conformational change of TCS accompanied with the membrane insertion was examined by measuring the CD and fluorescence spectra. The results showed that a pH-dependent intermediate exists in the protein-insertion process. A model illustrating the insertion process was set up based on the results.

MATERIALS AND METHODS

Materials

The following chemicals were purchased from Sigma (St. Louis, MO, U.S.A.): 1,2-dimyristoyl-*sn*-glycero-3-phosphocholine (DMPC), 1,2-dimyristoyl-*sn*-glycero-3-phosphoglycerol (DMPG), 1,2-dimyristoyl-*sn*-glycero-3-phosphoserine (DMPS), 1,2-dipalmitoyl-*sn*-glycero-3-phosphocholine (DPPC), 1,2-dipalmitoyl-*sn*-glycero-3-phosphoglycerol (DPPG), 1,2-distearoyl-*sn*-glycero-3-phosphoglycerol (DSPG), 2-(*p*-toluidino)naphthalene-6-sulphonic acid (TNS) and 1-anilinonaphthalene-8-sulphonic acid (ANSA). The other chemicals used were of analytical grade made in China.

Purification of TCS

TCS was extracted from the root of *T. kirilowii* (Tianhuafen) according to Zhang et al. [22] with slight modification. The dried slice of Tianhuafen obtained from a local drugstore was homogenized with 50 mM Tris/HCl buffer at pH 6.8 (buffer A) using a high-speed blender. The homogenate was centrifuged to remove insoluble material. Ammonium sulphate was added to 40 % saturation to the supernatant, and the mixture was left for 12 h and centrifuged. The collected supernatant was adjusted to 75 % saturation with ammonium sulphate, left for 6 h, and centrifuged

Abbreviations used: TCS, trichosanthin; RIP, ribosome-inactivating protein; DMPC, 1,2-dimyristoyl-*sn*-glycero-3-phosphocholine; DMPG, 1,2-dimyristoyl-*sn*-glycero-3-phosphoglycerol; DMPS, 1,2-dimyristoyl-*sn*-glycero-3-phosphoserine; DPPC, 1,2-dipalmitoyl-*sn*-glycero-3-phosphocholine; DPPG, 1,2-dipalmitoyl-*sn*-glycero-3-phosphoglycerol; DSPG, 1,2-distearoyl-*sn*-glycero-3-phosphoglycerol; TNS, 2-(*p*-toluidino)naphthalene-6-sulphonic acid; ANSA, 1-anilinonaphthalene-8-sulphonic acid.

[1] To whom correspondence should be addressed (e-mail suisf@mail.tsinghua.edu.cn).

again. The precipitate was resuspended with buffer A, and dialysed overnight against buffer A. The resulting solution was applied to a CM-Sepharose C-50 column, washed with buffer A, and eluted with buffer A containing 0.3 M NaCl. The elution peak was collected, and put on to the second column of Sephadex G-75, which was equilibrated with buffer A and eluted under the same conditions. TCS appeared in the second elution peak. Purity determination of TCS showed a single band of 27 kDa on SDS/PAGE (silver stained).

Preparation of phospholipid vesicles

Small unilamellar vesicles were prepared as follows: lipids of the desired composition were dissolved in chloroform/methanol (3:1, v/v) and dried under a stream of nitrogen. Residual solvents were removed under high vacuum for 2–3 h. The lipid films were then resuspended and sonicated in the desired buffer at 30 °C, by using a probe sonicator for approx. 2–3-min intervals to near optical clarity. The concentration of phospholipid was determined by phosphate analysis [23]. When lipid mixtures were used, appropriate aliquots of chloroform/methanol solution of each component were mixed and then dried together. Afterwards the homogeneous lipid mixture was dispersed in buffer and sonicated as usual.

Monolayer study

Monolayer surface pressure was measured using the Wilhelmy plate method [24] with a NIMA 9000 microbalance (Nima Technology Ltd, Coventry, U.K.). Surface pressure is defined as the surface-tension difference before and after the monolayer was spread on the solution surface. All the data were collected automatically and recorded by a personal computer.The home-made sample trough [25,26] had a volume of 4 ml and a surface area of 10 cm^2. The sub-phase was stirred continuously with a magnetic bar. During the experiment, the phospholipid was spread on the surface of the buffer to form a lipid monolayer. TCS was then injected into the sub-phase through a side sample hole after the surface pressure of the monolayer was steady. The pressure change was followed until it had reached a maximal value, which took about 1 h. All the experiments were carried out in N_2 to prevent the samples from being oxidized. The temperature of the system was controlled at 25 ± 0.5 °C.

Fluorescence measurements

Fluorescence was measured with a Hitachi M850 fluorescence spectrophotometer using a 1-cm^2 quartz fluorescence cuvette. The emission and excitation slit widths were set at 5 nm. The excitation wavelength was set at 387 nm for ANSA and 321 nm for TNS. The 400–600-nm emission spectrum was scanned for ANSA, while for TNS we only detected the emission intensity at 446 nm. The background spectra of the buffers were subtracted, and the data of the emission peaks and fluorescence intensities were determined from the corrected spectra.

CD spectroscopy

CD measurements were carried out on a Jasco J-715 spectropolarimeter. Samples containing TCS at a concentration of 0.5 μM with or without liposomes (200 μM) were scanned at least four times at the rate of 100 nm/min and averaged. The temperature of the sample compartment was maintained at 25 ± 0.2 °C with a circulating-water bath. The path length of the quartz cell was 0.2 mm. In the experiments, a blank run made with the liposome or buffer alone was subtracted carefully from the experimental spectra for correction. The 200–250-nm spectra were used for analysis and calculation because, in this wavelength range, the liposome scattering had little effect on the CD spectra. All spectra were smoothed and converted into the mean residue ellipticity, $[\theta]$, in degrees$\cdot cm^2 \cdot dmol^{-1}$, by using a mean residue molecular mass of 110 Da.

RESULTS

Effect of pH on TCS membrane insertion

Monolayer experiments were carried out to study the interactions between TCS and phospholipid. The monolayer surface-pressure increase ($\Delta\pi$) was followed after TCS was injected into the sub-phase. Since Demel et al. [27] established that agents known for interacting only with the phospholipid headgroup did not induce a surface-pressure increase in a monolayer, the surface-pressure increases of lipid monolayers after injection of proteins into the sub-phase are interpreted as the result of actual insertion of the proteins into the phospholipid monolayer. The results showed that for neutral phospholipids such as DPPC or DMPC, the surface-pressure increase caused by TCS insertion was undectectable. However, for negatively charged phospholipids (such as DMPS, DMPG or DPPG), TCS caused distinct surface-pressure increases. Further experiments in different pH environments revealed that TCS's membrane-insertion ability was influenced drastically by pH. For negatively charged DMPG, when the pH value was above 5.8, TCS did not cause an obvious membrane-surface-pressure increase. With decreasing bulk pH, TCS's interaction with negatively charged phospholipid increased until pH 4.6. In the pH range 4.6–5.8, TCS's membrane-insertion ability for negatively charged phospholipids exhibited an obvious pH-dependent characteristic (Figure 1). The monolayer experiment was described in detail in our previous work about TCS [21].

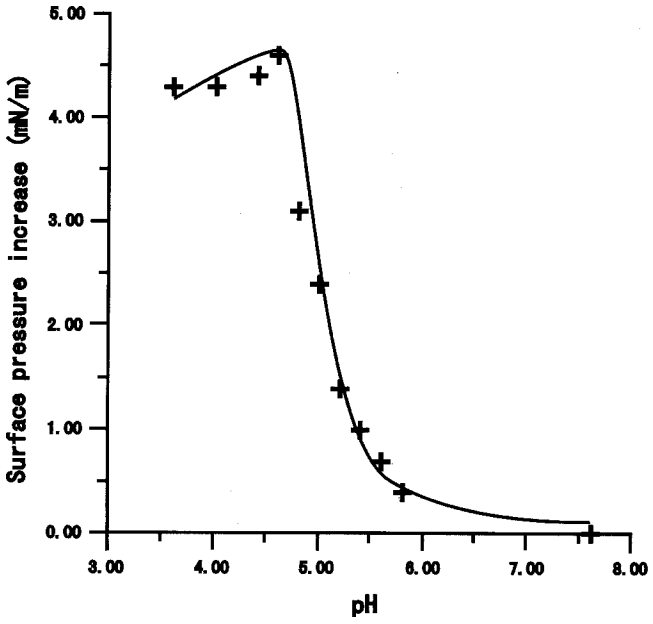

Figure 1 Influence of pH on TCS's insertion into DMPG monolayer

The initial monolayer pressures were kept at 20 ± 0.2 mN/m. The final concentration of TCS in the sub-phase was 200 nM. Tris/HCl (50 mM) buffer was used for pH 7.6, and 50 mM sodium acetate/acetic acid buffer was used for other pHs. The results were very similar for other phosphoglycerol lipids with different hydrophobic chains, such as DPPG and DSPG.

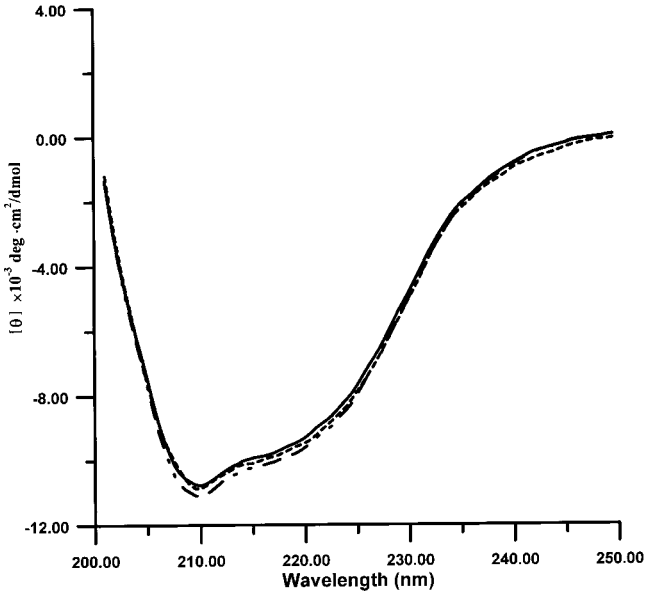

Figure 2 CD spectra of TCS at various pHs

Solid line, pH 5.8; dotted line, pH 4.6; dashed/dotted line, pH 3.0. Sodium acetate/acetic acid buffers (50 mM) were used for the three pHs. Samples containing TCS at a concentration of 0.5 μM were treated with the three pH buffers for 1 h before the experiment. The path length of the quartz cell was 0.2 mm. The experiment was carried out at 25 $\pm$ 0.2 °C.

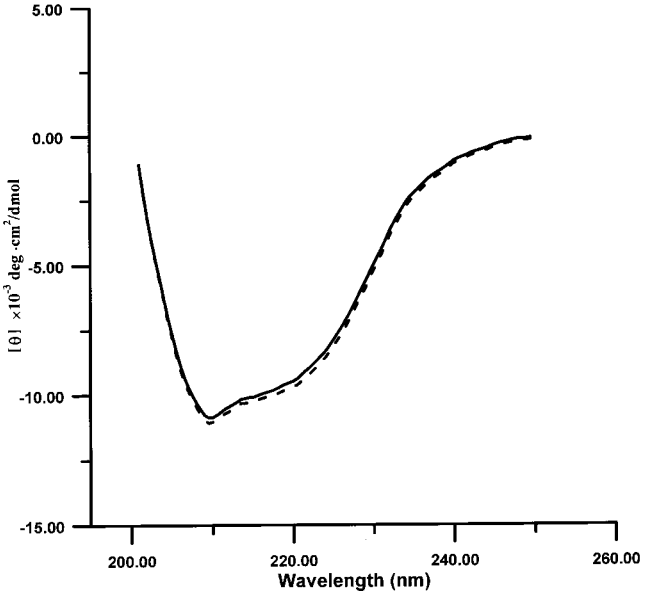

Figure 3 CD spectra of TCS with or without DMPG

Samples contained 0.5 μM TCS with (dotted line) or without (solid line) 200 μM DMPG liposomes. pH was kept at 4.6 for optimal membrane insertion. The path length of the quartz cell was 0.2 mm. The experiment was carried out at 25 $\pm$ 0.2 °C.

Table 1 The percentages of various secondary structures in TCS at different pHs with or without DMPG

The 200–240-nm spectrum was used for fitting. The fitting software used was J-700 for Windows Secondary Structure Estimate, version 1.10.00, provided by the JASCO Corporation, Hachioji City, Tokyo, Japan.

	Secondary structure (%)				
pH	α-Helix	β-Sheet	β-Turn	Random coil	Root mean square (%)
5.8	16.8	38.6	14.9	29.7	4.119
4.6	17.7	37.6	14.9	29.8	4.077
3.0	17.1	38.4	14.8	29.7	4.261
4.6, + DMPG	18.4	36.6	14.9	30.0	4.219

Effect of pH and membrane on TCS secondary structure

Membrane insertion of proteins is frequently accompanied by conformational change. If the secondary structure of TCS changes in the membrane-insertion process, it should be revealed by CD spectrosopy. So we used CD here to detect the secondary structure change of TCS in the membrane-insertion process. The CD (200–250 nm) of TCS in different-pH buffers is shown in Figure 2, and the contents of α-helices, β-sheets and β-coils were estimated by using the method programmed by Chang et al. [28]. The results indicated that TCS's secondary structure remained stable under various pH environments (Table 1).

The CD spectrum of TCS was also measured in the presence of DMPG liposomes. The experimental pH was set to 4.6 because this was proved to be the optimal pH for TCS insertion into DMPG membrane. Since quickly adding high concentrations of TCS may lead to the aggregation of the DMPG vesicles, TCS was added slowly to the liposomes (200 μM) to a final concentration of 0.5 μM and the sample solution maintained optical clarity during TCS addition. The CD (200–250 nm) results are shown in Figure 3 and the calculated results shown in Table 1.

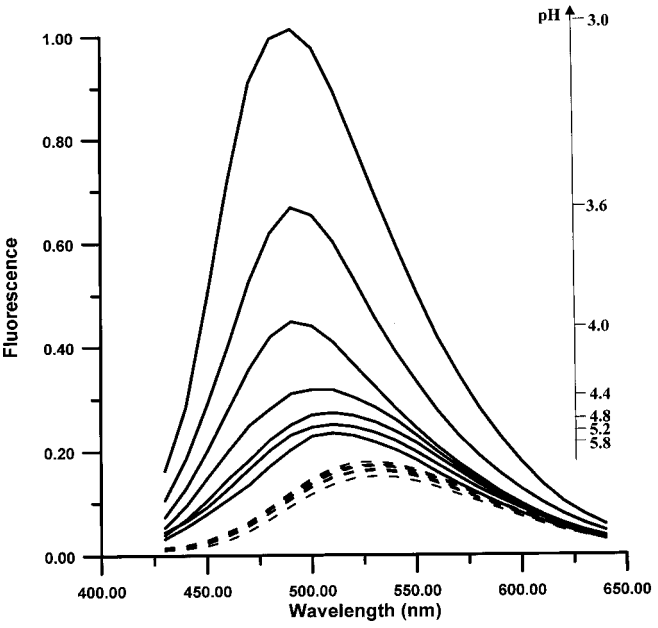

Figure 4 Effect of TCS on ANSA fluorescence under various pH conditions

ANSA was added to 2 μM TCS solutions at various pHs, and after 5 min the 420–650-nm spectrum was scanned while excited at 387 nm. The results are shown by solid lines. The pH decreased in the sequence of 5.8, 5.2, 4.8, 4.4, 4.0, 3.6 and 3.0 from bottom to top. The ANSA fluorescences at various pHs without TCS changed relatively little, as shown by the dashed lines. The experiment was carried out at 25 $\pm$ 0.2 °C.

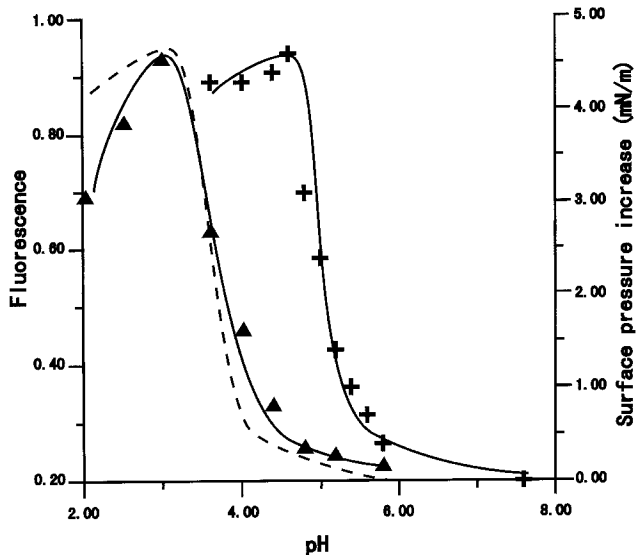

Figure 5 pH influence on TCS insertion and hydrophobic exposure

DMPG monolayer surface-pressure increase (+) and ANSA-fluorescence increase (▲) caused by TCS were plotted together against pH. The dashed curve was obtained by left-shifting the surface-pressure increase curve by 1.5 pH units, which is the pH gap between the membrane surface and the bulk in our experimental system. After the left shift, the *x* co-ordinate represents the pH at the membrane surface instead of the bulk pH. The three curves were adjusted arbitrarily to the same height for convenience.

pH-induced tertiary-structure change of TCS

The experiments described above have proved that TCS can insert into phospholipid membrane under appropriate conditions, but that its secondary structure remains stable. As we know, when a protein inserts into the lipid membrane, the hydrophobicity environment around it changes greatly, so it is very hard for a protein to insert into the membrane without conformational adjustment. Therefore it is possible that the protein undergoes tertiary-structure change in the membrane-insertion course. Since monolayer studies have proved TCS's membrane-insertion ability to be pH dependent, so this possible tertiary-structure change might also be pH dependent.

To test this, a fluorescence experiment was carried out using ANSA as probe. When excited at 387 nm, ANSA's fluorescence intensity is known to increase when binding to the hydrophobic sites of proteins [29]. So if it is added to the protein solution, the protein conformational change causing hydrophobic-site exposure should be reflected by the ANSA fluorescence. Experimental results showed that ANSA's fluorescence changed little in various pH buffers. But when ANSA was added into TCS solutions at various pHs, the fluorescence showed marked differences. Figure 4 shows that the fluorescence was much stronger when ANSA was added to the low-pH TCS solution, which suggested that more hydrophobic sites were exposed under these conditions. The fluorescence intensity against the pH of the solution is plotted in Figure 5. The shape of the resulting curve was very similar to the curve obtained in the monolayer experiment (Figure 1). When the two curves were plotted on one co-ordinate (Figure 5), we found that the fluorescence curve had a left-shift of about 1.6 pH units compared with the curve from the monolayer experiment.

Additionally, we found that low-pH-induced conformational change of TCS was a rather rapid process. When the pH-5.8 solution was adjusted to pH 3.0, and the ANSA fluorescence intensity was measured, the result showed that the fluorescence intensity increased instantly upon the lowering of pH, and the intensity retained stable for at least several hours.

pH difference between the membrane surface and the bulk

To explain the 1.6-pH-unit gap between the two curves mentioned above, we noticed that it has been pointed out that for negatively charged lipid membrane the surface pH differs from the bulk pH [30,31]. To test whether this pH difference caused the gap between our two curves, the surface pH of the DMPG membrane was measured in the following experiment.

According to Winiski et al. [32], binding of TNS is dependent on the surface potential of the lipid membrane, and the net fluorescence is proportional to the number of TNS molecules adsorbed to the membrane. The ratio of the probe molecules adsorbed to a charged surface to those adsorbed to a neutral surface is related to the membrane-surface electrostatic potential, ψ_0, by:

$$\psi_0 = (RT/F)\ln(f/f_0)$$

where f and f_0 are the net fluorescence intensities of TNS adsorbed to the charged and uncharged vesicles, respectively. The ψ_0 value can be used to calculate the ΔpH between the membrane surface and the bulk by the formula

$$\Delta\mathrm{pH} = \mathrm{pH}_{\mathrm{surface}} - \mathrm{pH}_{\mathrm{bulk}} = F\psi_0/(2.303\,RT).$$

Although Winiski et al. [32] have obtained ΔpH values for various DMPG/DMPC vesicles, these values were evidently dependent on the buffers used in their experiments, so their experiments were repeated using buffers identical to those used in our monolayer and fluorescence experiments. The result showed that for the various pH buffers used in our experiments, the ΔpH between the DMPG surface and the bulk was almost the same, with a value of about 1.5. When this ΔpH is considered, the ANSA fluorescence-experiment curve should be left-shifted by about 1.5 pH units, and the resulting curve superimposed over the monolayer-experiment curve quite well (shown in Figure 5). This suggested that the tertiary-structure change of TCS may be induced by the lower pH at the membrane surface, and this caused the hydrophobic-site exposure that might be important for the membrane insertion of TCS.

The optimal surface pH for TCS membrane insertion

As pointed out by Winiski et al. [32], the ΔpH between the membrane surface and the bulk is dependent on the charged-lipid portion of the membrane. For a DMPG/DMPC mixed-lipid membrane, the ΔpH value changes with the change of the percentage of DMPG (DMPG%). For membranes with lower DMPG%, to keep the membrane-surface pH equal, the bulk pH should be lower than for membranes with higher DMPG% values. So, if it is true that the membrane-surface pH and not the bulk pH directly influences the protein conformation, then for various DMPG/DMPC membranes the optimal bulk pH for TCS insertion into membranes with low DMPG% should be lower than that for membranes with relatively higher DMPG% values.

To test the above theory, the monolayer experiment was repeated using mixed DMPG/DMPC lipid with various DMPG% values. The resulting curves are plotted on one co-ordinate in Figure 6. The conclusion was drawn that with decreasing DMPG% in the mixed lipid, the optimal bulk pH for membrane insertion became lower. The optimal surface pHs for TCS insertion in various DMPG/DMPC membrane systems

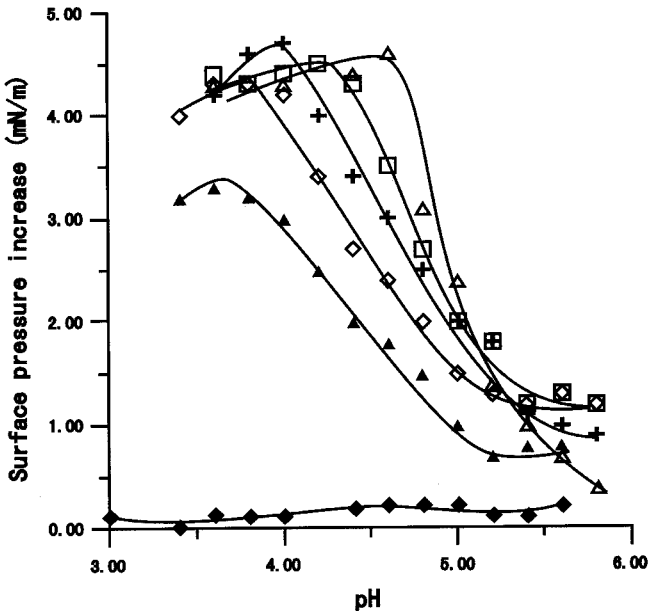

Figure 6 TCS membrane insertion in various DMPG/DMPC systems

The proportions of DMPG/DMPC were 1:0 (△), 2:1 (□), 1:1 (+), 1:2 (◇), 1:4 (▲) and 0:1 (◆). Experiments were carried out as described in Figure 1. The optimal pH for TCS insertion is defined as the pH at which TCS caused membrane surface pressure to reach its maximum.

Table 2 The pH decreasing at various DMPG/DMPC membrane surfaces

DMPG/DMPC ratio	pH decreasing at surface	Optimal bulk pH	Optimal surface pH
1:0	−1.5	4.6	3.1
2:1	−1.1	4.3	3.2
1:1	−0.9	4.0	3.1
1:2	−0.8	3.8	3.0
1:4	−0.5	3.6	3.1

were measured by the TNS method mentioned above. The result showed that for the various mixed lipids used, the optimal bulk pH for membrane insertion decreased with the decreasing of DMPG%, whereas the optimal surface pHs remained almost the same (Table 2). This optimal surface pH for membrane insertion had a value of about 3.0. This confirmed further that the membrane insertion of TCS was correlated with the low-pH-induced conformational change, and that the lower pH at the membrane surface may favour this conformational change.

DISCUSSION

The heterogeneous toxins from bacteria or plants usually act strongly on biological membranes. The well-studied toxins include colicin A, diphtheria toxin and ricin [33–35]. In most cases, the toxins can insert into the membrane and these membrane-insertion properties are thought to be important for their physiological effects. The results of the current work are very similar to those obtained for diphtheria toxin [36], which is also pH dependent. This pH-dependent character was thought to be essential for diphtheria toxin's toxicity, since it was supposed that diphtheria toxin enters the target cell by receptor-mediated endocytosis, followed by penetration through the membrane of an acidic organelle [37,38]. Defective acidification of the endosomes of the target cell may prevent the cells from being killed by the toxin [39]. For TCS, there is still no rigorous evidence demonstrating that it is endocytosed by the target cell. But since the membrane-insertion characteristic shown in this paper also represents a pH-dependent way, this may provide us with some indirect proof on its cell-entry path.

In the previous work on diphtheria toxin [36], Blewitt et al. pointed out that the toxins may aggregate under low-pH conditions, and this aggregation may give rise to various artifacts. But in our experiment, the gel-filtration result showed that the low-pH-treated and -untreated TCS appeared in the same elution volume, which indicated that no aggregation of the protein happened when treated with low pH (results not shown). So, no protein aggregation was considered when our experimental results were interpreted.

The monolayer experiment proved that the membrane-insertion ability of TCS was pH dependent, so the membrane-insertion-related conformational change of the protein might also be pH dependent. This was confirmed by the fluorescence experiment using ANSA as a probe. The major finding in this work is that the conformational change can be favoured by the membrane-surface pH, which is lower than the pH of the bulk. This is easy to understand because when a protein initiates its membrane-insertion course, it enters a special membrane-surface microenvironment. So the conformation of the protein is influenced directly by the membrane-surface pH instead of the bulk pH. Another piece of information from the fluorescence experiment is that the pH-induced conformational change will greatly enhance the ANSA fluorescence, which proves that there is hydrophobic-site exposure during the conformational change.

The conformational change happens only if the environment pH is low enough (the optimal pH value is 3.0), regardless of the other environmental factors. And this conformational change is a rather rapid process. So it can happen instantly after the protein enters the special membrane-surface microenvironment if the pH condition is met. Therefore, it is quite possible that the conformational change happens preceding the membrane-insertion course, and it is likely that the hydrophobic-site exposure caused by the conformational change initiates the membrane-insertion course.

One might ask why pH 3.0 is the optimal membrane-surface pH. We should point out that, in this paper, we focused on the optimal pH only because under this pH the experimental phenomena are their most distinct. In fact, the transition pH (under which the membrane-insertion ability of TCS reaches half of its maximum) may be more significant than the optimal pH. If the transition pH is considered, we find that for DMPG membrane, the transition membrane-surface pH is about 3.6, whereas the corresponding bulk pH is about 5.1, which is close to the pH found in endosomes [40,41].

In spite of the pH-induced conformational change, the electrostatic force between membrane and protein may also work in the insertion course. The following evidence supports this opinion: (i) for neutral phospholipid, such as DMPC, the membrane insertion was not observed even when the bulk pH was reduced to 3.0, which is sufficient for TCS conformational change; (ii) from Figure 6, when the surface-pressure increases under optimal pH (for convenience, we will call it maximal membrane-insertion ability, or I_{max}) was considered, we found that with the decrease of DMPG%, I_{max} remained unaltered at first, but it decreased obviously when DMPG% was decreased to 25%, so there might exist a saturant electric density needed for

the membrane insertion of TCS. Below this density, TCS membrane insertion will be restricted.

With all these results considered, a membrane-insertion model of TCS was proposed as the following. As a basic protein (pI 9.4), TCS carries positive charge when the pH is below its pI, so it can be adsorbed to negatively charged phospholipid membranes by electrostatic force and become enriched at the surface. The lower pH at the surface favours its conformational change and exposes its hydrophobic site, and this hydrophobic site may finally insert into the membrane due to hydrophobic force.

The importance of membrane-surface pH for protein insertion was reported by Van der Goot et al. in 1991 [42], and the protein-structure change with the secondary structure retained was described as a 'molten globular state' [43–45] in their work on colicin A. It may be a common rule that for proteins like colicin A and TCS, the secondary-structure units in their structures [46–48] are relatively stable and cannot be unfolded easily. In order to expose the hydrophobic sites, the 'molten globular state' is formed as a membrane-insertion precursor. Low pH may change the charges on some residues, which breaks the salt bridges and creates charge repulsions among the charged groups. These effects loosen the protein tertiary structure and cause the formation of the intermediate, and finally lead to membrane insertion.

This work was supported by the National Natural Science Foundation of China.

REFERENCES

1 Yeung, H. W., Wong, D. M., Ng, T. B. and Li, W. W. (1986) Purification of three isolations from root tubers of *Trichosanthes kirilowii* (Tian Hua Fen). Int. J. Pept. Protein Res. **27**, 325–333

2 Wang, Y., Qiang, R. Q., Gu, Z. W., Jin, S. W., Zhang, L. Q., Xia, Z. X., Tian, G. Y. and Ni, C. Z. (1986) Scientific evaluation of Tian Hua Fen (THF) history, chemistry and application. Pure Appl. Chem. **58**, 789–798

3 Cheng, K. F. (1982) Midtrimester abortion induced by *Radix trichosanthis*. Morphologic observations in placenta and fetus. Obstet. Gynecol. **59**, 494–498

4 Chan, Y., Tong, M. K. and Lau, M. J. (1982) Chinese and western style medicine for treatment of 238 cases of malignant hydatidiform mole. Shanghai J. Chin. Med. **3**, 30–31 (Chinese)

5 Law, L., Tam, P. P. L. and Yeung, H. W. (1983) Effect of α-momorchocin on the development of peri-implantation mouse embryos. J. Reprod. Fert. **69**, 597–604

6 Shaw, P. C., Chan, W. L., Yeung, H. W. and Ng, T. B. (1994) Trichosanthin - a protein with multiple pharmacological properties. Life Sci. **55**, 253–262

7 McGrath, M. S., Hwang, M. S., Caldwell, S. E., Gaston, I., Luk, K. C., Wu, P., Ng, V. L., Crowe, S., Daniels, J., Marsh, J. et al. (1989) GLQ223: an inhibitor of human immunodeficiency virus replication in acutely and chronically infected cells of lymphocyte and mononuclear phagocyte lineage. Proc. Natl. Acad. Sci. U.S.A. **86**, 2844–2848

8 Ferrari, P., Trabaud, M. A., Rommain, M., Mandine, E., Zalisz, R., Desgranges, C. and Smets, P. (1991) Toxicity and activity of purified trichosanthin. AIDS **5**, 865–870

9 Zhao, J., Ben, L. H., Wu, Y. L., Hu, W., Ling, K., Xin, S. M., Nie, H. L., Ma, L. and Pei, G. (1999) Anti-HIV agent trichosanthin enhances the capabilities of chemokines to stimulate chemotaxis and G protein activation, and this is mediated through interaction of trichosanthin and chemokine receptors. J. Exp. Med. **190**, 101–111

10 Byers, V. S., Levin, A. S., Malvino, A., Waites, L., Robins, R. A. and Baldwin, R. W. (1994) A phase II study of effect of addition of trichosanthin to zidovudine in patients with HIV disease and failing antiretroviral agents. AIDS Res. Hum. Retroviruses **10**, 413–420

11 Mayer, R. A., Sergios, P. A., Coonan, K. and O'Brien, L. (1992) Trichosanthin treatment of HIV-induced immune dysregulation. Eur. J. Clin. Invest. **22**, 113–122

12 Byers, V. S., Levin, A. S., Waites, L. A., Starrett, B. A., Mayer, R. A., Clegg, J. A., Price, M. R., Robins, R. A., Delaney, M. and Baldwin, R. W. (1990) A phase I/II study of trichosanthin treatment of HIV disease. AIDS **4**, 1189–1196

13 Kahn, J. O., Kaplan, L. D., Gambertoglio, J. G., Bredesen, D., Arri, C. J., Turin, L., Kibort, T., Williams, R. L., Lifson, J. D. and Volberding, P. A. (1990) The safety and pharmacokinetics of GLQ223 in subjects with AIDS amd AIDS-related complex: a phase I study. AIDS **4**, 1197–1204

14 Li, M. X., Yeung, H. W., Pan, L. P. and Chan, S. I. (1991) Trichosanthin, a potent HIV-1 inhibitor, can cleave supercoiled DNA *in vitro*. Nucleic Acids Res. **19**, 6309–6312

15 Zhang, X. J. and Wang, J. H. (1986) Homology of trichosanthin and ricin A chain. Nature (London) **321**, 477–478

16 Collins, E. J., Robertus, J. D., Lopresti, M., Stone, K. L., Williams, K. P., Kwang, K. and Piatak, M. (1990) Primary amino acid sequence of alpha-trichosanthin and molecular models for abrin A-chain and alpha-trichosanthin. J. Biol. Chem. **265**, 8665–8669

17 Zhang, J. S. and Liu, W. Y. (1992) The mechanism of action of trichosanthin on eukaryotic ribosomes - RNA N-glycosidase activity of the cytotoxin. Nucleic Acids Res. **20**, 1271–1275

18 Wu, S., Lu, X. H., Zhu, Y. R., Yang, J. and Dong, Y. C. (1998) N-glycosidase mechanism of trichosanthin. Sci. China Ser. C. Life Sci. **41**, 174–180

19 Hu, V. W. and Holmes, R. K. (1984) Evidence for direct insertion of fragments A and B of diphtheria toxin into model membranes. J. Biol. Chem. **259**, 12226–12233

20 Beaumelle, B., Alam, M. and Hopkins, C. R. (1993) ATP-dependent translocation of ricin across the membrane of purified endosomes. J. Biol. Chem. **268**, 23661–23669

21 Xia, X. F., Wang, S. X., Luo, J. B., Wong, R. N. S. and Sui, S. F. (1999) Trichosanthin can spontaneously penetrate phospholipid monolayer under acid condition. Chinese Sci. Bull. **44**, 1892–1895

22 Zhang, Y., Li, W. L., Hao, Q., Yu, G., Li, Q. S. and Yao, Q. Z. (1993) Tb(III) and Eu(III) as fluorescence probes to investigate the metal-binding sites of trichosanthin. Biochem. Biophys. Res. Commun. **197**, 407–414

23 Ames, B. N. (1966) Assay of inorganic phosphate, total phosphate and phosphatases. Methods Enzymol. **8**, 115–118

24 Demel, R. A. (1974) Monolayers-description of use and interaction. Methods Enzymol. **32**, 539–545

25 Han, X. H., Sui, S. F. and Yang, F. Y. (1996) A mini-trough for the study of membrane insertion ability of proteins. Thin Solid Films **284–285**, 789–792

26 Wang, S. X., Cai, G. P. and Sui, S. F. (1998) The insertion of human apolipoprotein H into phospholipid membranes: a monolayer study. Biochem. J. **335**, 225–232

27 Demel, R. A., London, Y., Geurts van Kessel, W. S. M., Vossenberg, F. G., van Deenen, L. L. et al. (1973) The specific interaction of myelin basic protein with lipids at the air-water interface. Biochim. Biophys. Acta **311**, 507–519

28 Chang, C. T., Wu, C. C. and Yang, J. T. (1978) Circular dichroic analysis of protein conformation: inclusion of the beta-turns. Anal. Biochem. **91**, 13–31

29 Stryer, L. (1965) The interaction of a naphthalene dye with apomyoglobin and apohemoglobin, A fluorescent probe of non-polar binding sites. J. Mol. Biol. **13**, 482–495

30 Eisenberg, M., Gresalfi, T., Riccio, T. and Mclaughlin, S. (1979) Adsorption of monovalent cations to bilayer membranes containing negative phospholipids. Biochemistry **18**, 5213–5223

31 Menestrina, G., Forti, S. and Gambale, F. (1989) Interaction of tetanus toxin with lipid vesicles, effects of pH, surface charge, and transmembrane potential on the kinetics of channel formation. Biophys. J. **55**, 393–405

32 Winiski, A. P., McLaughlin, A. C., McDaniel, R. V., Eisenberg, M. and McLaughlin, S. (1986) An experimental test of the discreteness-of-charge effect in positive and negative lipid bilayers. Biochemistry **25**, 8206–8214

33 Pattus, F., Martinez, M. C., Dargent, B., Cavard, D., Verger, R. and Lazdunski, C. (1983) Interaction of Colicin A with phospholipid monolayers and liposomes. Biochemistry **22**, 5698–5703

34 Beaumelle, B., Bensammar, L. and Bienvenue, A. (1992) Selective translocation of the A chain of diphtheria toxin across the membrane of purified endosomes. J. Biol. Chem. **267**, 11525–11531

35 Beaumelle, B., Alami, M. and Hopkins, C. R. (1993) ATP-dependent translocation of ricin across the membrane of purified endosomes. J. Biol. Chem. **268**, 23661–23669

36 Blewitt, M. G., Chung, L. A. and London, E. (1985) Effect of pH on the conformation of diphtheria toxin and its implication for membrane penetration. Biochemistry **24**, 5458–5464

37 Draper, R. K. and Simon, M. I. (1980) The entry of diphtheria toxin into the mammalian cell cytoplasm: evidence for lysosomal involvement. J. Cell Biol. **87**, 849–854

38 Sandvig, K. and Olsnes, S. (1980) Diphtheria toxin entry into cells is facilitated by low pH. J. Cell Biol. **87**, 828–832

39 Merion, M., Schlesinger, P., Brooks, R. M., Moehring, J. M., Moehring, T. J. and Sly, W. S. (1983) Defective acidification of endosomes in Chinese hamster ovary cell mutants 'cross-resistant' to toxins and viruses. Proc. Natl. Acad. Sci. U.S.A. **80**, 5315–5319

40 Geisow, M. J. and Evans, W. H. (1984) pH in the endosome, measurements during pinocytosis and receptor-mediated endocytosis. Exp. Cell Res. **150**, 36–46

41 Maxfield, F. R. (1982) Weak bases and ionophores rapidly and reversibly raise the pH of endocytic vesicles in cultured mouse fibroblasts. J. Cell Biol. **95**, 676–681

42 Van der Goot, F. G., Gonzalez-Manas, J. M., Lakey, J. H. and Pattus, F. (1991) A 'molten-globule' membrane insertion intermediate of the pore-forming domain of colicin A. Nature (London) **354**, 408–410

43 Ptitsyn, O. B., Pain, R. H., Semisotov, G. V., Zerovnik, E. and Razgulyaev, O. I. (1990) Evidence for a molten globule state as a general intermediate in protein folding. FEBS Lett. **262**, 20–24
44 Goto, Y., Takahashi, N. and Fink, A. (1990) Mechanism of acid-induced folding of proteins. Biochemistry **29**, 3480–3488
45 Ewbank, J. J. and Creighton, T. E. (1991) The molten globule protein conformation probed by disulphide bonds. Nature (London) **350**, 518–520
46 Gao, B., Ma, X. Q., Wang, Y. P., Chen, S. Z., Wu, S. and Dong, Y. C. (1994) Refined structure of trichosanthin at 1.73Å resolution. Sci. China Ser. B **37**, 59–73
47 Pan, K. Z., Lin, Y. J., Zhou, K. J., Fu, Z. J., Chen, M. H., Huang, D. R. and Huang, D. H. (1993) The crystal and molecular structure of trichosanthin at 2.6Å resolution. Sci. China Ser. B **36**, 1069–1081
48 Parker, M. W., Pattus, F., Tucker, A. D. and Tsernoglou, D. (1989) Structure of the membrane-pore-forming fragment of colicin A. Nature (London) **377**, 93–96

Received 7 January 2000/25 April 2000; accepted 18 May 2000